ORIGINAL RESEARCH PAPER

Microstructure and Swelling Behaviour of Poly (Acrylamide-co-Acrylic Acid) based Nanocomposite Superabsorbent Hydrogels

Sasan Ganjehie; Ahmad Gholizadeh*; Seyed Ahmad Ketabi

School of Physics, Damghan University (DU), Damghan, Iran

ABSTRACT

In this paper, microstructure and swelling behavior of five superabsorbent hydrogels have been investigated. These samples were prepared by dispersing watermelon shell powder (WSP) and cucumber shell powder (CSP), mixture bentonite and WSP, mixture bentonite and CSP, zeolite (Z) bentonite (B), into poly(acrylamide-co-acrylic acid) (P) backbone in an aqueous medium. The nanocomposites have been synthesized through chemical cross-linking by polymerization technique using N,N-methylenebis acrylamide as a cross-linker and potassium persulfate as an initiator in simple aqueous environmental conditions. The nanocomposite hydrogels named as P-WSP-CSP، P-WSP-B، P-CSP-B, P-Z, P-B, respectively. These superabsorbent nanocomposites were characterized by X-ray diffraction, Fourier transforms infrared and field emission-scanning electron microscope measurements. The water absorption and desorption of the superabsorbent nanocomposites have also been studied. Our findings show that very high water absorption and lower drying rate of P-CSP-B are attributed to higher porous surfaces observed in FE-SEM images. The results show the superabsorbent hydrogels based on CSP represent very high water absorbency capacity and water retention ability that make them suitable for technology applications.

Keywords: *Chemical Cross-Linking Method, Nanocomposite, Structural and Surface Properties, Superabsorbent, Water Absorption and Retention*

© 2018 Published by Journal of Nanoanalysis.

INTRODUCTION

In recent years, there has been considerable interest in water-swellable superabsorbent polymers that are suitable for absorbing and holding a large amount of water while maintaining its physical dimensional structure. The superabsorbent is a three-dimensional network contain a large number of hydrophilic functional groups of hydrophilic polymers held together by cross-links of covalent bonds or ionic and or secondary forces in the form of hydrogen bonds or hydrophobic interactions [1-4]. Polymer gels are further processed by copolymerization of a monomer and a grid in a solvent or by inserting cross-linker into a heterogeneous polymer solution. The ability of hydrogels to absorb water arises from various mechanisms including dispersal process, osmotic mechanism and from hydrophilic functional groups attached to the polymeric backbone while their resistance to dissolution arises from cross-links between network chains [5].

The dependence of superabsorbent polymers on the water makes them useful in technology, especially for the agriculture, health products, industrial adsorbents, medicine and cosmetics [6]. Also, exceptional properties of superabsorbents such as biocompatibility, biodegradability, renewability, and non-toxicity make them acceptable for application in agricultural activities. Polymerization of acrylate monomers onto polysaccharides is an efficient

* Corresponding Author Email: *gholizadeh@du.ac.ir*

method for the preparation of the superabsorbent polymer. The superabsorbent forming ability through polymerization of monomers onto polysaccharides such as chitosan, sodium alginate, starch, cellulose, xanthan gum and carrageenan has been well documented [7,8].

Watermelon shell Powder (WSP) and Cucumber shell Powder (CSP) are renewable, biodegradable, non-toxic, biocompatible [9], and sustainable low-cost polysaccharides. Its wide application is limited by a number of the structural and performance characteristics (e.g., poor water solubility at room temperature) [10]. However, by grafting monomers of acrylic acid and acrylamide to the WSP (or CSP) and WSP (or CSP)-based hydrogels can effectively combine the properties of both polysaccharides and synthetic polymers. Hydrogels based on WSP and CSP are a kind of advanced polymer material with good salt resistance, high mechanical strength, water absorbency, and water retention.

In this paper, the synthesis and characterization of organic-mineral superabsorbent nanocomposites for controlled release applications have been reported. Then, microstructural properties and swelling of organic-organic polymeric nanocomposites composed of poly(acrylamide-co-acrylicacid)- WSP (or CSP) through chemical cross-linking by polymerization technique using N, N'-methylenebisacrylamide as a cross-linker and potassium persulfate as an initiator are studied under simple aqueous environmental conditions. Also to improve the mechanical properties of such superabsorbent polymers, we used method compounding poly(acrylic acid)/poly(acrylamide)- WSP (or CSP) with inorganic clays (Montmorillonite). Adding inorganic clay is a relatively effective method to improve the properties of this type of hydrogel [11]. The results have shown that the addition of adequate amounts of inorganic clays could improve the mechanical strength and water absorbing capability of the Super absorbent. In this study, nanocomposite polymers were characterized by XRD, FTIR and FE-SEM measurements. There are no reports on these nanocomposite polymers so far.

EXPERIMENTAL
Materials
Both monomers Acrylamide and Acrylic acid (AA, Merck, 99%) needed for the synthesis of Poly(acrylic acid)/Poly(acrylamide)- WSP (or CSP) superabsorbent were neutralized up to

80% with NaOH in an ice bath. Non-neutralized potassium persulfate (Merck) as the initiator and N, N'-methylenebisacrylamide (Merck) as the cross-linker was then used. WSP and CSP obtained from fresh watermelon and cucumber were dried using an oven dryer for 24 hours at 50°C and then sieved on 200 mesh sieve. Deionized water and high pure nitrogen gas were used during polarization process.

Synthesis of the superabsorbent polymers
Initially, 2 grams of acrylamide dissolved in 30 mL of distilled water were transferred to a 250 mL balloon with WSP (or CSP or ratio 1:1 of bentonite and CSP or ratio 1:1 of bentonite and WSP)) to prepare acrylamide-WSP, acrylamide-CSP, acrylamide-WSP-bentonite, and acrylamide-WSP-bentonite. This balloon is a round bottom flask with three necks (a thermometer, mixer, and $N_2(g)$ entries). To prepare the homogeneous solution and the exclusion of oxygen, the mechanical stirring was carried out throughout the reaction under a slow flow of nitrogen for an hour. Acrylic acid (10 mL) was dissolved in 10 mL distilled water and also neutralized to 80% with NaOH in an ice bath. Then, 14 mL of neutralized acrylic acid and acrylamide-WSP (acrylamide-CSP, acrylamide-WSP-bentonite, and acrylamide-WSP-bentonite) were added to the required amount of potassium persulfate (0.38g) dissolved in 2 mL of distilled water. After 15 min., a required amount of N, N'-methylenebisacrylamide (0.032g) dissolved in distilled water was added to the mixture. Afterward, the mixture was kept in a water bath at 70°C to complete polymerization. The mechanical stirring was carried out throughout the reaction. After complete polymerization, the resulting product was washed with ethanol for 5 minutes and, finally dried at 40°C for 15 hours. For convenience, the abbreviations of poly(acrylamide-co-acrylicacid)-WSP, poly(acrylamide-co-acrylicacid)-CSP, poly(acrylamide-co-acrylicacid)- WSP-bentonite and poly(acrylamide-co-acrylicacid)-CSP-bentonite are selected as P-WSP, P-CSP, P-WSP-B and P-CSP-B.

Characterization
Infrared spectra of the superabsorbents were recorded on a Perkin Elmer 2 RX1 FTIR instrument using the KBr pressed disk technique over the spectral range between 400 and 4000 cm^{-1}. The dried samples were blended with a ratio of 1 to 100 with KBr powder and pressed into tablets before spectrum acquisition. The X-ray powder

diffraction of the superabsorbents was obtained using a Bruker X-ray diffractometer with Cu-Kα radiation (λ=1.54048Aᵒ) source over an angle range of 2θ = 5-75° and a resolution of 0.02. Surface morphology images of synthesized superabsorbent nanocomposites were analyzed by Field-Emission Scanning Electron Microscope (FE-SEM, HITACHI S-4160 model).

For evaluation of water absorbency in the samples, a pure and dry hydrogel sample was placed in 500 mL of ionized water for 210 minutes. After equilibrium, residual water was removed by filtration and holding up for 45 minutes. The water absorption capacity of the samples versus time was calculated as the weight of the water absorbed per gram of the superabsorbent polymers as follows [12,13].

$$Q_{eq} = (M_2 - M_1)/M_1 \qquad (1)$$

where M_1 and M_2 are the weights of the dry sample and the swollen sample, respectively. Q_{eq2} was calculated as grams of water per gram of sample (g/g). In this way, the swelling rate of the samples synthesized under various stages and conditions was measured. The values of water retention were obtained by following equation:

$$\% \, W.R. = (M_t/M_o) \times 100 \qquad (2)$$

where M_0 is the initial weight of the superabsorbent in water and M_t is the weight after the loss of water at each time interval.

RESULTS AND DISCUSSIONS

The results of FTIR spectroscopy of the samples are shown in Fig. 1. In general, various oxygen functional groups in the structure include the vibration modes of epoxy (C–O-C) (1230–1320 cm⁻¹), sp2- C=C (1500–1600 cm⁻¹, in-plane vibrations), carboxyl (COOH) (1650–1750 cm⁻¹), carbonyl species (C=O) (1600–1650 cm⁻¹; 1750–1850 cm⁻¹), C-H and hydroxyl (C–OH) (3050–3800 cm⁻¹ and 1070 cm⁻¹) with all C–OH vibrations from COOH and H_2O.

The following functional groups are identified in FTIR spectra of the superabsorbents: the absorption bands at 3660 cm⁻¹ and 3450 cm⁻¹ were owing to the stretching vibrations of the hydroxyl group (OH) due to the presence of acid or water in the samples; bands at 1725 cm⁻¹ related to C=O; the adsorption band at approximately 1535 cm⁻¹ corresponds to the C=C bonding of aromatic rings; 500 cm⁻¹, 1435 cm⁻¹ belonging to group stretching vibration C-OH; C-O vibration at 795 cm⁻¹, and 1050 cm⁻¹ and 1265 cm⁻¹ are due to aromatic anti-symmetrical coupled epoxy stretching of sp² hybridized molecules (C-O) and (C-C) bonding [14]. Just below 3000 cm⁻¹ are two peaks CH₃

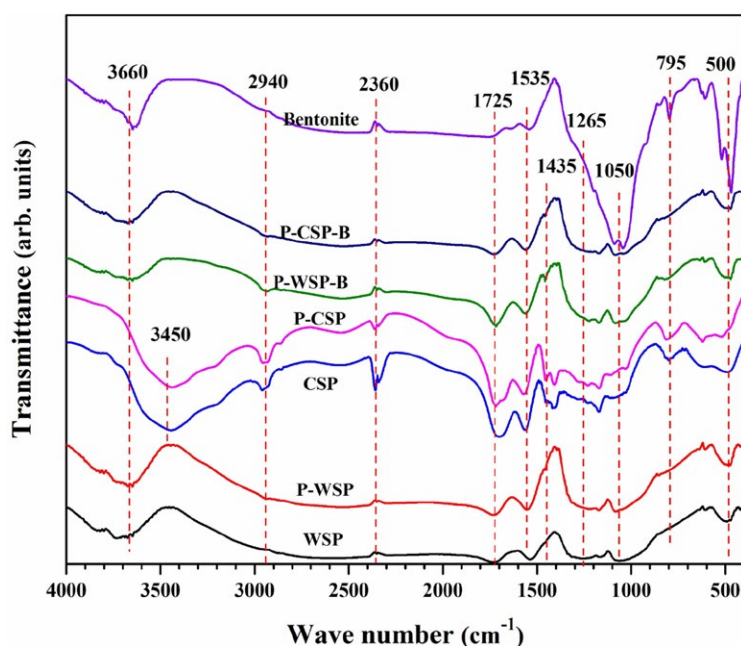Fig. 1. FTIR spectra of WSP, P-WSP, P-WSP-B, CSP, P-CSP, P-CSP-B and bentonite.

(2940 cm^{-1}) and CH$_2$ (2920 cm^{-1}). The peak at 2940 cm^{-1} and 2920 cm^{-1} are from CH$_3$ asymmetric and CH$_2$ asymmetric stretching vibration. The bond at around 2360 cm^{-1} is assigned to CO$_2$ originated from the air during FTIR measurement. The appearance of the hydroxyl group (OH) at lower wave number for CSP and P-CSP can contribute to increase in higher water absorbency.

The XRD patterns of the superabsorbent polymers are shown in Fig. 2. They also had similar phenomena except for WSP. The peak broadening and weakness indicate the disordered intercalated structure. This peak observed in superabsorbents indicate that poly(acrylamide-co-acrylicacid) is dispersed at the molecular level in WSP and CSP matrix. Also, the position of the diffraction peak of the superabsorbents was significantly different from that of the WSP and CSP. The XRD pattern of WSP shows major peaks at diffraction angles 2θ = 28.27, 40.52, 50.33 and 66.50º indicating that the WSP is semi-crystalline in nature. The XRD pattern of P-WSP shows broadens peak at 19.8º. This indicated that the hydrogels had no crystallinity. The polymer segments grafted onto the active sites of the WSP, can limit the mobility of the WSP molecules and interfere with their ability to form an ordered structure; the regularity of the WSP molecular chains was destroyed. Loss of crystallinity of the hydrogels was detected

in the XRD patterns in Singh's studies on the synthesis of microwave-accelerated grafting of potato starch with acrylamide [15], which are typical for amorphous polymers. In the XRD pattern of the superabsorbents, a prominent peak is corresponding to the basal spacing occurred at about 2θ = 20º in WSP and CSP, but in superabsorbent polymers occurred at about 2θ = 22º. It reflects the intercalation of poly(acrylamide-co-acrylicacid) into the WSP and CSP sheets via polymerization process, moves the basal reflection of WSP and CSP to a higher angle which in turn, confirms the formation of composites.

The FE-SEM micrographs of P-WSP, P-CSP, P-WSP-B and P-CSP-B nanocomposite polymers are shown in Fig. 3. The FE-SEM image of the P-WSP shows a multilayer structure with the rough and dense surface, while P-CSP has a porous matrix structure (see Figs. 3(a) and 3(b)). Since porosity size is related to the rate of water absorption because the penetration of water into the reinforced polymeric network is convenient. Therefore, P-CSP polymer and composites containing P-CSP should have a relatively high water absorption rate. The presence of much more porosity on the surface of P-CSP with respect to P-WSP can contribute to a high water absorbency for this sample. As seen in Fig. 3 (c) for P-WSP-B, the superabsorbent based on the combination of bentonite and P-WSP has a
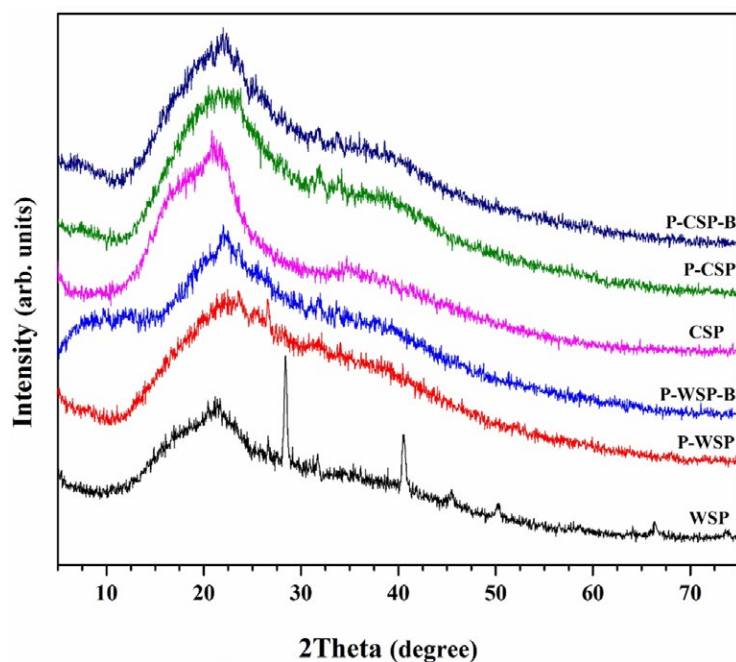

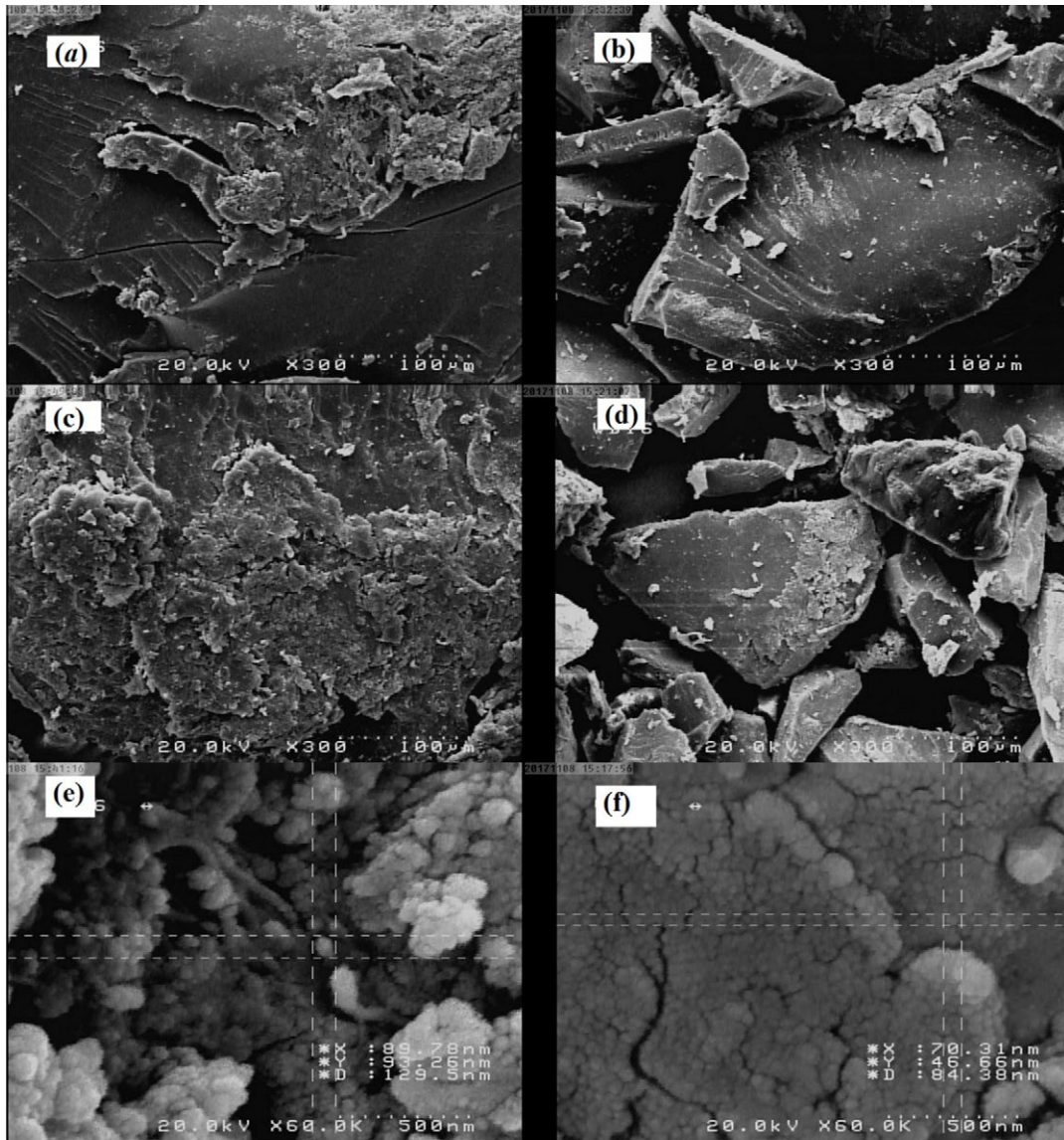Fig. 2. XRD patterns of WSP, P-WSP, P-WSP-B, CSP, P-CSP, and P-CSP-B.

Fig. 3. FE-SEM micrograph of (*a*) P-WSP, (b) P-CSP, (c) P-WSP-B and (d) P-CSP-B nanocomposite polymers in scale 100μm. (e) and (f) are P-WSP-B and (d) P-CSP-B nanocomposite polymers in scale 500nm, respectively.

compact layer structure like P-WSP. However, in FE-SEM image of P-CSP-B (Figs. 3(d), 3(f)), the bentonite particles distributed in P-CSP matrix form a superabsorbent nanocomposite.

Fig. 4 shows the swelling kinetic curve of the produced hydrogels at a time period of 210 minutes**.** The results indicate that all nanocomposites show an increase in swelling up to 100 minutes of immersion in water and then further increase of immersing time had no evident influence on water absorbency of the superabsorbent. This phenomenon, namely the superabsorbent firstly swelled to a maximum value following by a gradual

deswelling until the equilibrium, is actually known as the overshooting effect, which can be interpreted as the consequence of a swelling-deswelling process [6]. The water absorbency of the samples P-CSP and P-CSP-B are much more than the other ones. The ability of P-CSP and P-CSP-B to absorb water arises from the hydrophilic functional groups attached to the polymeric backbone of CSP while the resistance of P-WSP-B to dissolution arises from cross-links between network chains due to the presence of bentonite. The highest swelling rate 5025 ± 5 (g/g) observed for the hydrogel polymer containing P-CSP and bentonite that is higher than
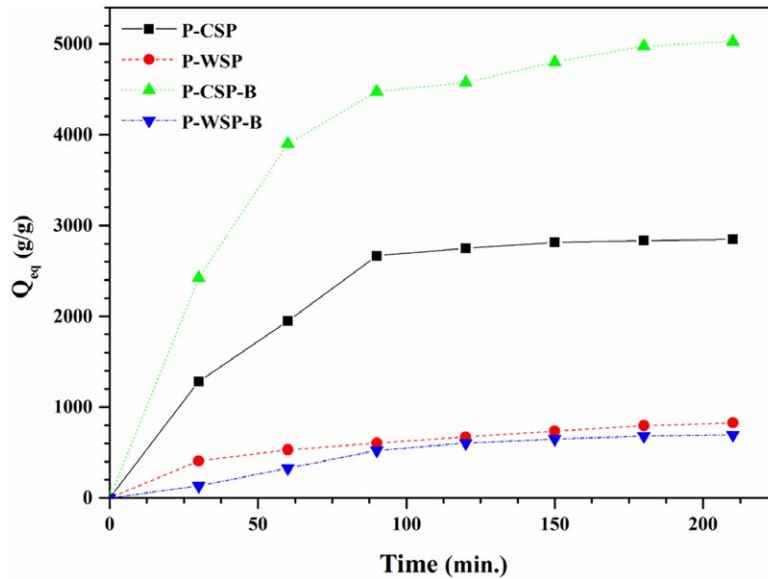
Fig. 4. Water absorption graph of P-WSP, P-CSP, P-WSP-B and P-CSP-B nanocomposite polymers.
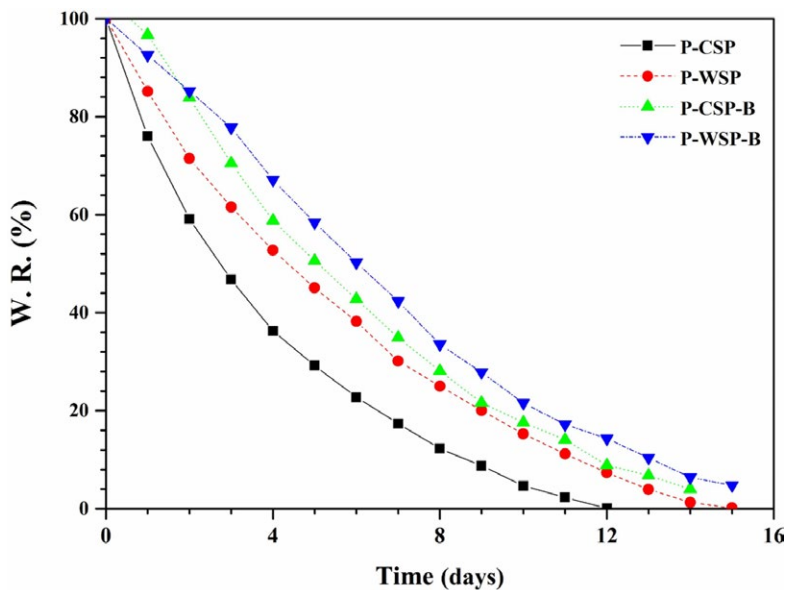

Fig. 5. Water retention graph of P-CSP, P-WSP, P-CSP-B and P-WSP-B polymers.

the values reported among other superabsorbent studied earlier [15, 6]. The presence of bentonite can increase the porosity of P-CSP and consequently contribute to higher water absorbency.

In Fig. 5, the water retention graph of the samples is presented. Superabsorbents P-CSP and P-CSP-B have shown higher drying rate compared to superabsorbent based on P-WSP. This may be due to an increased porosity as

evident by the SEM micrograph, thereby showing an increased desorption of liquid from the samples. As seen in Fig. 5, a long time interval of 12 days for water desorption of P-CSP and 15 days in P-WSP-B have been evaluated. This desorption process time can also be increased in the soil environment, which makes the performance of these superabsorbents suitable for agriculture and microfibrillated cellulose.

CONCLUSION

In this paper, structural, surface morphology, water absorption and water desorption properties of four superabsorbent polymers named P-WSP, P-CSP, P-WSP-B, and P-CSP-B have been investigated. The interpenetrating network hydrogels were prepared by dispersion of WSP or CSP-bentonite into poly(acrylamide-co-acrylic acid) backbone in an aqueous medium using the chemical cross-linking method. The XRD patterns of the samples show a prominent peak corresponding to the basal spacing occurred at about $2\theta = 22^\circ$ which is typical for amorphous polymers. The different oxygen functional groups identified in FTIR spectra thereby forming the superabsorbent composites can contribute to the ability of hydrogels to absorb water. FE-SEM investigation reveals that the superabsorbent polymer based on CSP exhibit a porous surface that can improve equilibrium water absorbency capacity and water retention ability. While the resistance of superabsorbents based on WSP to dissolution is attributed to rough and dense surfaces observed in FE-SEM images. The results of the water absorbency in the superabsorbents indicate that the water absorption rate of 5025 ± 5 g/g in P-CSP-B is much more than superabsorbent P-WSP-B with absorption rate 700 ± 5 g/g. These samples have shown lower drying rate that which makes the performance of these superabsorbents suitable for technology applications, especially the agriculture and the novel drug delivery.

CONFLICT OF INTEREST

The authors declare that there is no conflict of interests regarding the publication of this manuscript.

REFERENCES

[1] M. Ahmed Enas, J. Adv. Res., 6, 105 (2015).

[2] F. Aida and M. Fall., MINER. ENG., 50, 38 (2013).

[3] W.E. Hennink, N. Van, Adv. Drug Del. Rev., 54, 13 (2002).

[4] Absorbency and superabsorbency. Modern superabsorbent polymer technology, L. Buchholz Fredric and A. T. Graham, 1997, Wiley-VCH, New York, p.1-18.

[5] T. Ozbolat Ibrahim and M. Hospodiuk, Biomaterials, 76, 321 (2016).

[6] A. Bhattacharya, Sh. Sankar, A. Mishra, D. Pal, A. K. Ghosh, A. Ghosh, S. Banerjee and K. K. Sen, Polym.-Plast. Technol. Eng., 51, 878 (2012).

[7] H. Hosseinzadeh, A. Pourjavadi, M. Zohuriaan, J. Biomater. Sci. Polym. Edn., 15, 1499 (2005).

[8] A. Pourjavadi, M. Zohuriaan, G.R. Mahdavinia, Polym. Adv. Technol., 15, 173 (2004).

[9] G. Feng, B.-Zh. Li, H. Xia, B. Adhikari and Q. Gao, Carbohydr. Polym., 115, 605 (2015).

[10] G. Qiaoxia, Y. Wang, Y. Fan, X. Liu, Sh. Ren, Y. Wen and B. Shen, Carbohydr. Polym., 117, 247 (2015).

[11] Ch. Chunyu et al., Eur. Polym. J., 46, 92 (2010).

[12] B. Subham, L. Siddiqui, Sh. S. Bhattacharya, S. Kaity, A. Ghosh, P. Chattopadhyay, A. Pandey and L. Singh, Int. J. Biol. Macromol., 50, 198 (2012).

[13] V. L. Finkenstadt and J.L. Willett, MACROMOL. CHEM. PHYS., 206, 1648 (2005).

[14] B. Rafiei, and F. Ahmadi Ghomi, Iran. J. Crystallogr. Mineral., 21, 25 (2013).

[15] V. Singh, A. Tiwari, S. Pandey and K. Singh K, Starch-starke, 58, 536 (2006).